

Unmanned Aircraft Vehicle Autopilot Using Genetic Algorithm for Minimizing Blank Spot

Ronny Mardiyanto¹, Muhammad Ichlasul Salik², Djoko Purwanto³

Abstract—This paper presents the autopilot of unmanned aerial vehicles (UAV) with the ability to minimize blank spots on aerial mapping using the genetic algorithm. The purpose of the developed autopilot is to accelerate the times required for aerial mapping and save battery consumption. Faster time in conducting aerial mapping saves operational costs, saves battery consumption, and reduces UAV maintenance costs. The proposed autopilot has the ability to analyze blank spots from aerial shots and optimize flight routes for re-photography. The genetic algorithm was applied to obtain the shortest distance, which was done to save battery consumption and flight time. When developing the autopilot, the operator would manually set the flight route, then the aircraft would fly according to that route. The unstable wind factor has caused a shift in the flight route, which correspondingly caused blank spots. After all flight routes were traversed, the system developed would analyze the location of the blank spots. The new flight route was calculated using the genetic algorithm to determine the shortest distance from all the blank spot locations. The system developed consisted of a UAV equipped with autopilot and a ground control station (GCS). At the time of flight, the UAV would send the coordinates of the path traversed to the GCS to calculate the blank spot analysis. After the flight mission has been completed, the GCS would create a new route and send it to the UAV. The test carried out was an aircraft with a height of 120m using a 4S 4,200 mAh 25C lipo battery, and the percentage of throttle when flying straight was 30%. The results obtained are that the developed autopilot saves 46.4% of the time and saves 41.18% of battery capacity compared to conventional autopilots.

Keywords—Autopilot, Aerial Mapping, Blank Spot, Genetic Algorithm, Optimization, Time, Distance.

I. INTRODUCTION

Currently, the unmanned aerial vehicle (UAV) is rapidly developing and utilized in various fields. The UAV technology eases previously challenging works, such as in the extra high voltage transmission lines (SUTET) inspection. Moreover, this technology allows the operator to control it remotely so it can be used for aerial monitoring or photography function. The advantages of the UAV include increased revenue (due to the reduced operational cost) and decreased accident risks.

The UAV discussed in this paper is the aerial photography UAV to generate a map (photogrammetry). Before the UAV technology was invented, aerial photography was conducted by

renting a passenger aircraft and then manually taking the photos. Using UAV technology, aerial photography is carried out by placing a high-resolution camera in a UAV. The usage of the UAV for aerial photography provides more benefits as its costs are lower than those of a passenger aircraft rental. In addition, the mission execution time becomes more effective and efficient. The UAV usage also enables aerial photography in a narrow area. It can fly over 300 meters above sea level to avoid cloud disturbance [1].

In taking aerial photography, the operator will initially arrange the UAV's flight route according to the mapping plan to be carried out. Then, the UAV will fly as per the route (waypoint) [2]. However, external interference factors (such as wind) can cause the UAV's flight route to shift from the determined route. The different wind speeds from a particular direction will also affect the actual flight route. Consequently, aerial photography will not come out immaculately because of blank spots (areas where the photography is unsuccessful). In aerial photography using a UAV, a high-resolution camera replaces an expensive camera designed specifically for aerial photography [3]. Aerial mapping using fixed-wing UAV has also been conducted and has many benefits [4]. A very well-known autopilot product to control UAV is Pixhawk [5].

The genetic algorithm has been extensively used for travel salesman problem (TSP). This algorithm applies a primary concept that the most superior will survive while the weak will be extinct [6]-[8].

This research developed an autopilot capable of re-flying with the flight route passing through the blank spots. The distance optimization was carried out using the genetic algorithm method. Due to the use of the genetic algorithm in optimization, the mileage is getting shorter. It correspondingly leads to faster flying time and re-photography. Hence, the economic advantage will be obtained since aerial photography is cheaper and quicker, considering that one aerial photography location can be completed only in one flight.

II. UAV'S FLIGHT ROUTE PLANNING

Research on UAV's routes has been massively conducted. The UAV automatization development for flight route planning has been carried out using the genetic algorithm [9]. This method used a master-slave parallel vector-evaluated genetic algorithm (MSPVEGA). The results achieved suggest that this algorithm requires a large population and generation. Great population size is needed to gather information; at the same time, the number of a generation affects the speed.

The optimization has been conducted by combining several algorithms, namely a genetic algorithm, simulated annealing, and targeted mutation [10]. The benefits offered by the genetic algorithm are parallelism and global optimization, while the

^{1,2,3} Department of Electrical Engineering, Institut Teknologi Sepuluh Nopember, Gedung B, C & AJ Kampus Institut Teknologi Sepuluh Nopember, Keputih, Kec. Sukolilo, Kota SBY, Jawa Timur 60111 (telp 031-5947302; ¹ronny.mardiyanto@gmail.com, ²muhammadichlasulsalik@gmail.com, ³djoko@ee.its.ac.id)

[Received: 23 December 2021, Revised: 11 January 2022]

drawbacks lie in the low speed and ease of getting caught in the local optimum. The advantage of the simulated annealing algorithm is that it is more reliable in avoiding the local optimum trap. Meanwhile, the targeted mutation algorithm has the benefits of increasing genetic variation and accelerating the process of finding solutions. The collaboration between genetic algorithms, simulated annealing, and targeted mutations can accelerate the achievement of global optimum and inhibit prematurity.

The genetic algorithm has been improved by applying operator immune, which consists of vaccination and immune selection [11]. Vaccination modifies several genes in individuals, while immune selection compares fitness values for individual offspring and both parents in deciding which individuals will survive. The addition of an immune operator effectively increases the convergence speed and prevents prematurity.

The UAV route planning has already been done using the vibrational genetic algorithm [12]. The low population rate and short generation cycle are the advantages of this method. Implementing a vibrational mutation operator causes individuals to spread. Therefore, it is possible to avoid escaping from the local optimum condition and reach the global optimum quickly. A vibrational mutation operator also leads to higher mutation, random individual distribution, and elitism allows individual distribution to stay in the right direction.

The UAV's flight route planning to avoid forbidden zones has been carried out using the genetic algorithm [13]. This system avoids forbidden zones by producing a flight route with the shortest distance.

In this paper, the genetic algorithm was used to create a new flight route that would repair blank spot zones caused by the UAV's failures to traverse the route due to weather factors. The process of creating the new route was done in real time after all planned flight routes were carried out by the autopilot. Due to its ease of being executed using a microcontroller with a low processor speed, the genetic algorithm was then selected for optimization.

III. THE DEVELOPED AUTOPILOT

A conventional autopilot system is shown in Fig. 1. At first, the operator arranged the flight route according to the area which would be photographed. Next, the UAV would take off and take aerial photography while flying as per the arranged route. After the entire route was traversed, the aircraft would land. In the offline mode, images taken would be undergoing a stitching process. Results of the image stitching process were analyzed manually to determine the presence of blank spots. Then, blank spot locations were used for the new flight route and the UAV would fly for the second time. These steps were carried out iteratively until all blank spots disappeared. This paper improves the conventional method by simply doing one flight. In doing so, the UAV would analyze blank spots while flying and immediately carry out flight planning automatically. Steps of flight route planning are shown in Fig. 2, the system illustration developed is presented in Fig. 3, and the autopilot system developed is shown in Fig. 4.

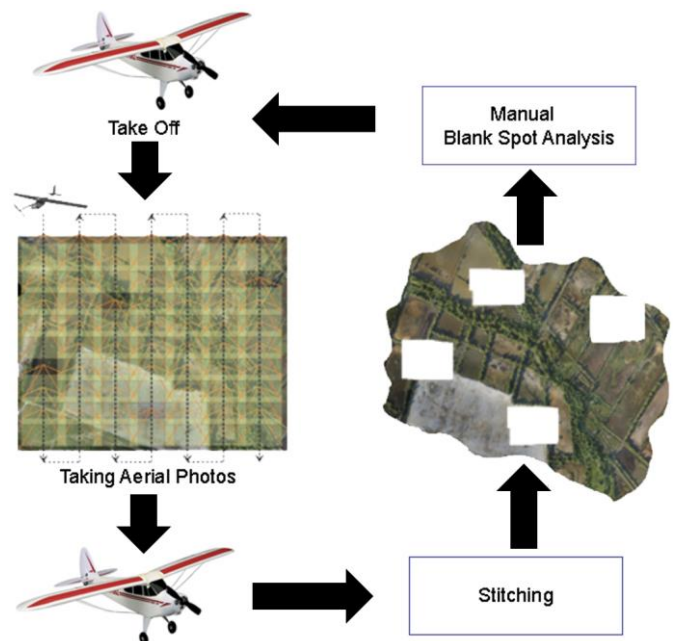


Fig. 1 Conventional autopilot system.

The difference between the conventional aerial mapping system and the proposed one lies in the conventional system. The blank spot identification process is conducted manually and coercing the UAV to land first; on the contrary, in the proposed system, the blank spot identification process is done while the aircraft is still in the air. The developed autopilot has essential additional functions, namely an automatic blank spot analysis and an effective new flight route arrangement using genetic algorithms. The whole system process sequence began with the operator entering the flight route by taking into account the coverage of the photography area. The planned flight route was uploaded to the autopilot through the ground control station (GCS). After conducting a pre-flight check and meeting all the flight parameters, the aircraft would take off. Subsequently, the UAV entered auto mode, flew according to the determined route, and took aerial photography. The entire aircraft's data (including GPS coordinates, altitude, position, and other parameters) was sent to GCS; then, it continuously recorded GPS coordinates to analyze blank spots. Once all flight routes were traversed, the autopilot would directly analyze blank spots according to GPS coordinates sent to GCS. The new flight route was made in accordance with the blank spot coordinates that underwent distance optimization using the genetic algorithm. After that, the UAV executed the new flight route until no blank spots were detected. When the mission was completed, the landing was performed using return to launch (RTL) mode. The aerial mapping process could be completed more quickly and reduce operational costs by employing the proposed system.

A. Blank Spots Analysis in Flying Condition

The developed autopilot continuously sent GPS coordinates that the UAV traversed to GCS. Subsequently, GCS analyzed blank spots and determined the new flight route optimized using the genetic algorithm.

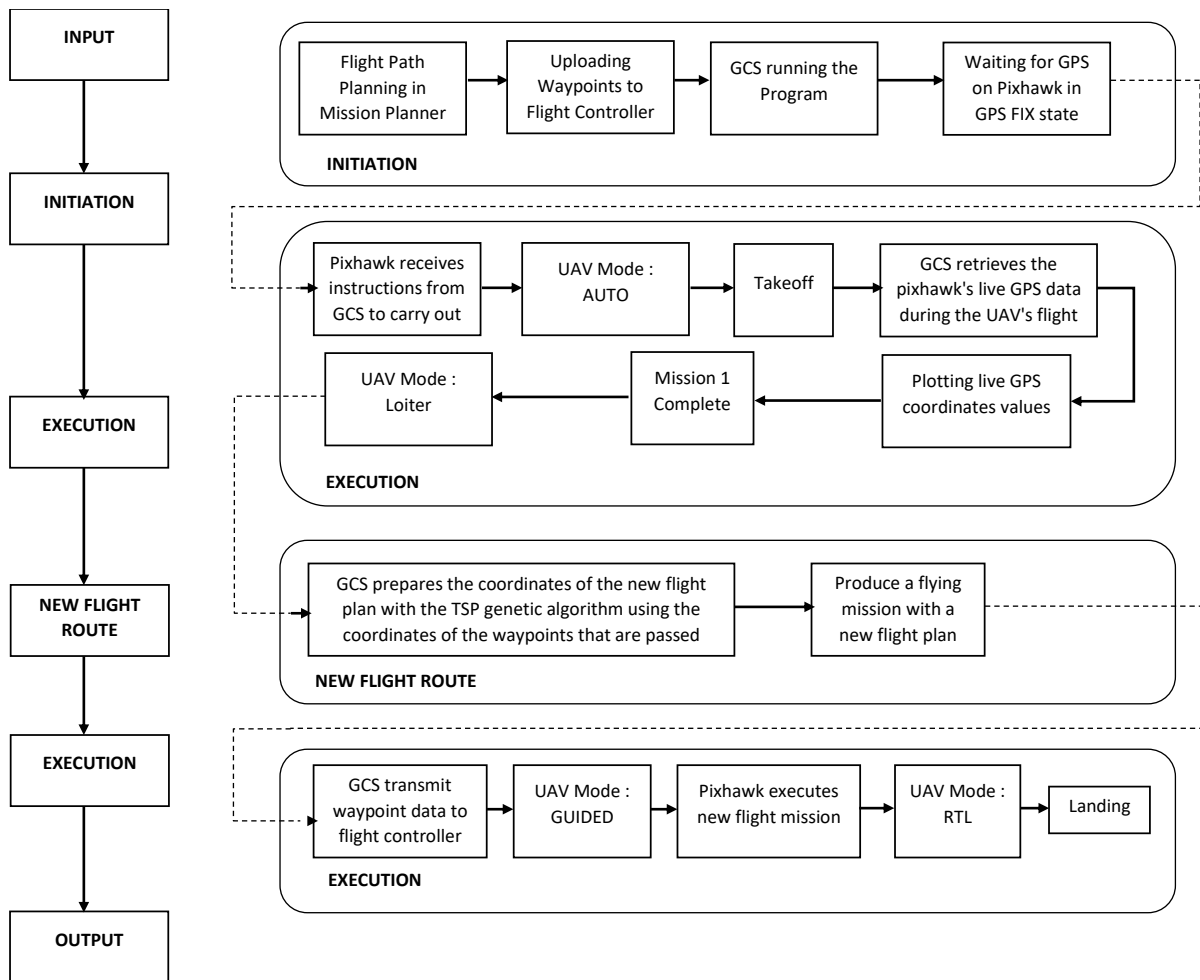


Fig. 2 Proposed system block diagram.

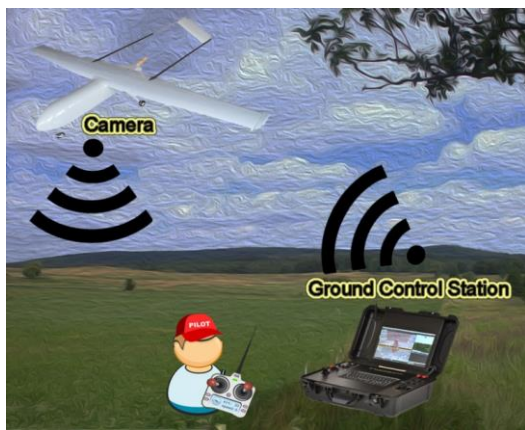


Fig. 3 Illustration of the GCS system.

B. Camera Coverage Calculation

The specifications of the camera used are shown in Table I. The calculation of the coverage area in an aerial mapping photo was carried out using the ground sampling distance (GSD) [14].

$$GSD \text{ (cm/pixel)} = \frac{\text{Sensor Width (mm)} \times \text{Flight Height (m)} \times 100}{\text{Focal Length (mm)} \times \text{Image Width (pixel)}} \quad (1)$$

$$GSD = \frac{6.08 \text{ mm} \times 100 \text{ m} \times 100}{2.73 \text{ mm} \times 4,608 \text{ pixel}} = 4.83 \text{ cm/pixel}$$

The area value of each photo is as follows.

$$\text{Height (m)} = \text{Image Width (pixel)} \times GSD \quad (2)$$

$$\text{Height} = 4,608 \text{ pixel} \times 4.83 \text{ cm/pixel} = 222.71 \text{ m}$$

$$\text{Width (m)} = \text{Image Height (pixel)} \times GSD \quad (3)$$

$$\text{Width} = 3,456 \text{ pixel} \times 4.83 \text{ cm/pixel} = 167.03 \text{ m}$$

$$\text{Area value (m}^2\text{)} = \text{Height(m)} \times \text{Width (m)}$$

$$\text{Area value} = 222.71 \times 167.03 = 37,200.01 \text{ m}^2$$

C. Blank Spot Zone Analysis Mechanism

The stage of analyzing the presence of blank spot zones was done by the depiction of the photography area coverage represented by a blue rectangle image. The center point originated from the conversion value of the earth coordinates of the UAV position into a canvas coordinate in a canvas image which area was adjusted to the scale of the total mapping coverage area. The blue rectangle's size was adjusted to the camera's coverage area in a photo according to the GSD

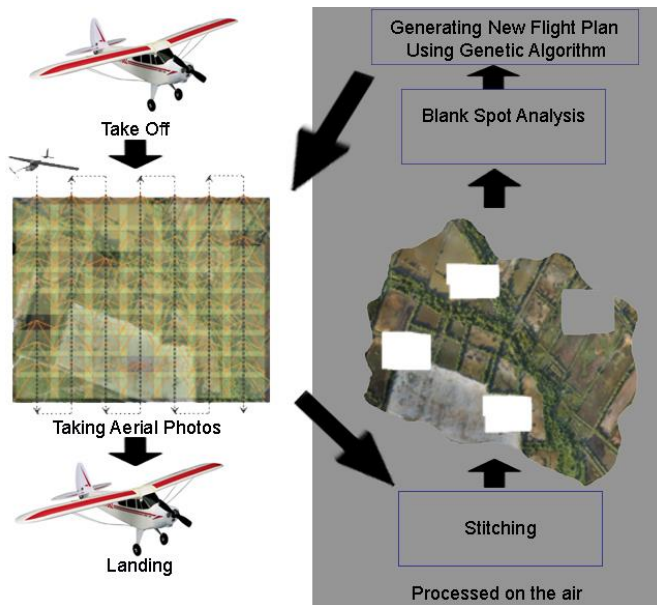


Fig. 4 Autopilot system development.

TABLE I
SPECIFICATIONS OF THE CAMERA USED

No	Parameter	Values in Xiaomi Yi Cam
1	Focal length	2.73
2	Pixel size	1.12
3	Flight altitude	100
4	Sensor width	6.08
5	Sensor height	4.56
6	Image width	4,608
7	Image height	3,456

calculation. In Fig. 5, dots represent coordinates of UAV position successfully recorded by GCS; the blue rectangle, on the other hand, is the coverage area calculated using the GSD formula.

The following stage was conducting the plotting process of the blue rectangle on the canvas. The center point was adjusted to the coordinates of the successfully recorded UAV positions, which results are shown in Fig. 6. This stage continued until the UAV completed the flight mission so that, in the end, it resulted in canvas images covered with blue rectangles. As presented in Fig. 7(b), the UAV has successfully photographed the entire desired area if the entire canvas image turns blue. Meanwhile, red-colored images on the canvas, shown in Fig. 7(a), indicate that the area in question is not photographed or not entirely traversed by the UAV during the flight mission.

After that, the results of the canvas depiction were analyzed using the OpenCV function, namely the blob analysis method. This analysis generated the coordinates of blank spot zones, as depicted in Fig. 8. The coordinate data were coordinates of areas that were indicated as blank spot zones. These coordinate data were eventually optimized using the genetic algorithm to obtain the UAV flight route arrangement used to execute the entire coordinates. As a result, the shortest total mileage was obtained.

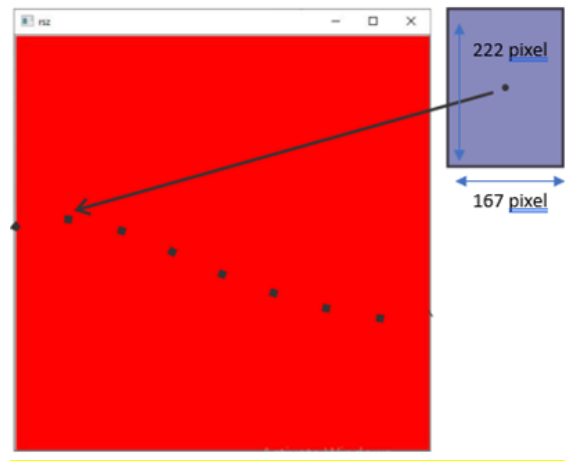


Fig. 5 Illustration of the photography coverage plotting mechanism.

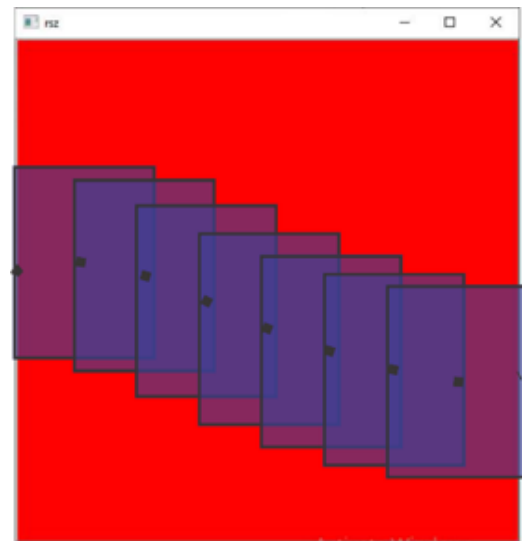


Fig. 6 Illustration of plotting mechanism results.

D. Creating a New Distance-Optimized Flight Route Using the Genetic Algorithm

The process that followed the blank spot analysis was creating the new distance-optimized route using the genetic algorithm. This step was conducted to make the UAV fly only once during the mapping mission, which was more timesaving and eventually reduced operational costs. At this stage, the autopilot made the re-photography process effective and efficient. It could be achieved once the UAV battery capacity could be maximized, which was directly proportional to the distance traveled by the UAV. The process of creating the new flight route used the genetic algorithm with blank spot coordinates as the input. The stages of implementing the genetic algorithm are as follows.

1) *Coding*: The gene used was the blank spot coordinates. The coordinates were coded using decimal numbers. The coding was based on the data order received from the previous analysis results.

2) *Population Generation*: The population was generated using the random method. Population size was adjusted to the

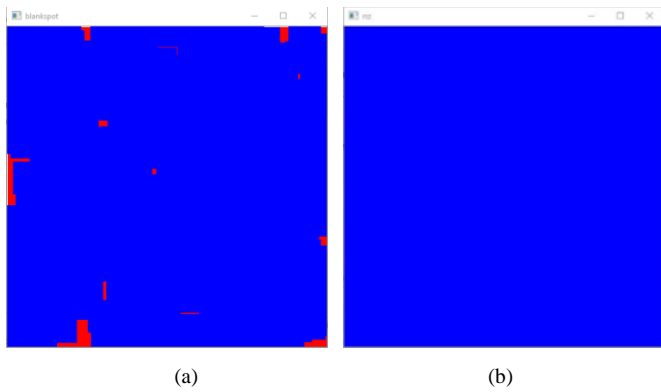


Fig. 7 Canvas, (a) with blank spot zones, (b) without blank spot zones.

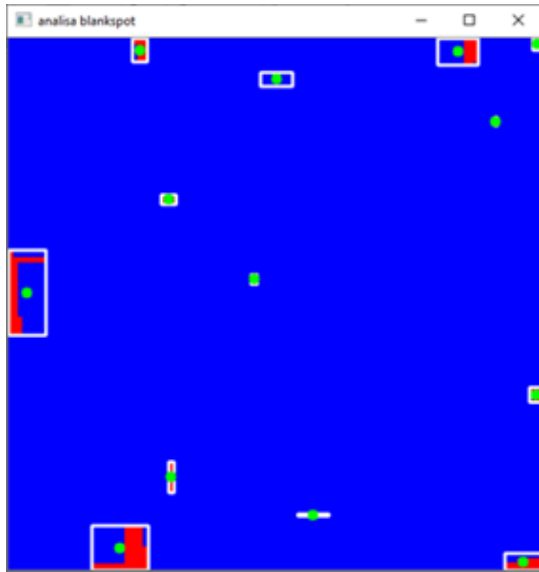


Fig. 8 Results of applying blank spot zone analysis on a canvas.

needs. Generating this population would provide many solution vectors.

3) *Evaluation*: An evaluation was applied to the generated solution to measure the suitability level of the solution vector to the goal solution. The evaluation was performed using the fitness function. It was carried out at this stage by calculating the total distance from the generated solution. Then, the fitness function value was calculated using (4).

$$f(x) = \frac{1}{distance^{8+1}} \quad (4)$$

The results of this stage were the solution vector with the shortest distance, so that it had a greater fitness function value.

4) *Elitism*: After obtaining a solution vector that was considered good, the elitism stage was conducted to maintain the best individual. Individuals deemed good would remain and replace those with the lowest fitness function values in the population.

5) *Crossbreeding*: This stage generated a new individual by crossbreeding two individuals. This process was done by combining pieces of genes from one parent with a different parent.



Fig. 9 UAV assembly result.



Fig. 10 Ground control station.



Fig. 11 Flight route pattern.

6) *Mutation*: Mutations resulted in new individuals that were not the result of crossbreeding.

7) *Repetition*: The repetition was carried out continuously until the expected objective function was achieved.

Of all the stages of genetic algorithms, the result was the coordinates of a new distance-optimized flight route.

IV. TESTING AND ANALYSIS

The developed autopilot was realized and underwent flight testing. The UAV and GCS used for the testing purpose are shown in Fig. 9 and Fig. 10. An autopilot test was conducted with and without optimization to measure the autopilot's capabilities.

The UAV specification used was a fixed-wing type with a wingspan of 1.2 m. The autopilot hardware used was the Pixhawk APM Plane with Arduplane firmware. The camera used for photography was the Xiaomi Yi Cam, while the GPS



Fig. 12 result of stitching mission 1.

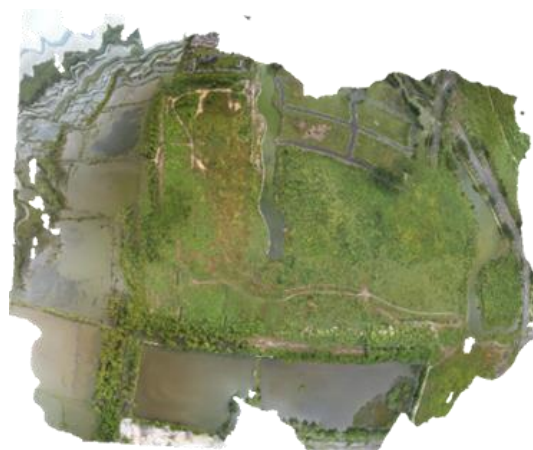


Fig. 14 Stitching results of combining mission 1 and mission 2 photos.

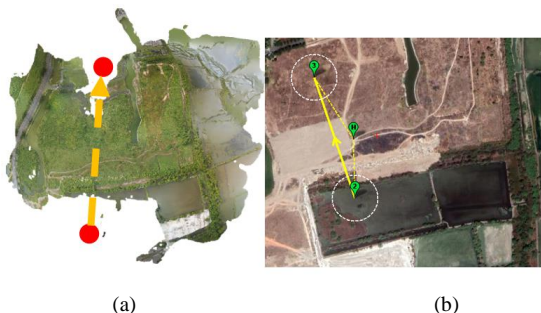


Fig. 13 A follow-up flight planning, (a) illustration of flight routes resulting from blank spot analysis, (b) implementation of the second flight route.

TABLE II
STITCHING PROCESS TIME USING THE FIRST MISSION CONVENTIONAL AUTOPILOT

Order	Stage	Quality	Time (s)
1	Align photos	Low	321
2	Build dense cloud	Low	234
3	Build mesh	Low	240
4	Build texture	Low	80
5	Build tiled model	Low	1,560
6	Build orthomosaic	Low	305
7	Export orthomosaic		321
Total time			2,777

used was the Ublox Neo M8n. The battery used was a Lipo 4S 4,200 mAh 25C and the percentage of throttle when flying straight was 30%.

A. Autopilot Testing without Optimization

In this testing, the UAV conducted the aerial mapping using a conventional system without distance optimization. The mapping was carried out on an area of 500 m × 500 m (area = 2,500 m²) in Pakuwon City, Surabaya. The flight route planning was set by sidalap (overlapping photos between adjacent flights to the side) of 0%, resulting in a horizontal flight distance of 255 m. The overlap value (overlapping photo to the front) was set based on the time-lapse of the camera, which was 2 s. The UAV was flown at an altitude of 120 m and the waypoint radius of 50 m. A flight route with these parameters would produce a route as shown in Fig. 11. Several

TABLE III
STITCHING PROCESS USING A CONVENTIONAL AUTOPILOT ON MISSION 2

Order	Stage	Quality	Time (s)
1	Align photos	Low	436
2	Build dense cloud	Low	384
3	Build mesh	Low	287
4	Build texture	Low	117
5	Build tiled model	Low	1,500
6	Build orthomosaic	Low	390
7	Export orthomosaic		33
Total time			3,147

TABLE IV
TIME REQUIRED FOR MAPPING USING A CONVENTIONAL AUTOPILOT SYSTEM

No	Activity	Required Time (s)
1	First flight	141
2	Second flight	68
3	First Stitching	2,777
4	Second stitching	3,147
Total time		6,133

times, the flight was carried out until all the blank spots were gone.

In Fig. 11, the straight lines represent the flight routes, the white dotted circles represent the waypoint radius, the dotted straight lines are the direction to Home (H), and the numbers indicate the waypoint sequence. This testing took 141 s. The mission resulted in photos as many as seventy photos with a photo size of 16 MP. These photos were then processed with Agisoft Photoscan Professional software to generate a map presented in Fig. 12. The result shows several imperfect areas (blank spots) caused by a shift in the flight route. The time used for the stitching process with the conventional autopilot on the first mission is presented in Table II.

In the conventional system, a follow-up flight was required to fix the blank spots. The planning of this flight route was determined based on the analysis result of the first flight's stitching process, as shown in Fig. 13.

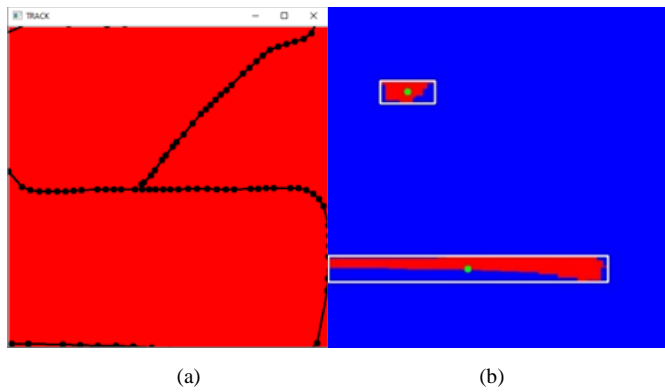


Fig. 15 Results of the autopilot testing with optimization, (a) record results of the UAV flight route, (b) analysis result of blank spot zones.

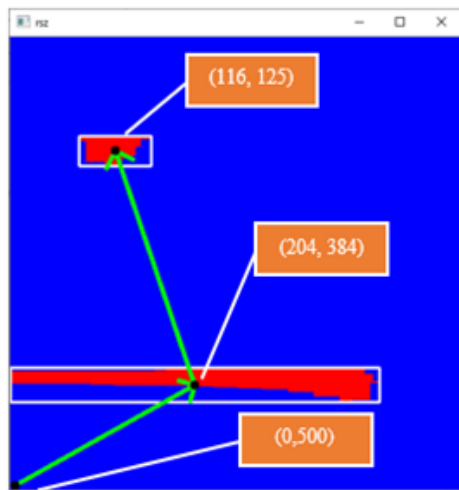


Fig. 16 Flight route from the result of the genetic algorithm implementation.

TABLE V

VARIABLE VALUES IN THE IMPLEMENTATION OF THE GENETIC ALGORITHM

Variable	Information
Number of populations	30 chromosomes
Elitism	2 chromosomes
Mutation percentage	30%
Number of repetitions	100

The second flight took 68 s and generated 34 photos. The results of the second flight underwent the stitching process to be combined with the results of the first flight, as shown in Fig. 14. The results of the second flight suggest that the map can be improved according to the desired mapping area. The stitching process time using conventional autopilot for the second mission is shown in Table III.

The testing conducted indicates that the conventional system requires a minimum of two flights to generate a perfect map. The first flight was performed as per the planned mission, whereas the second flight sought to correct the data obtained from the first flight. Table IV presents the total time calculation; the required battery capacity for all flights is 3,570 mAh.

B. Autopilot Testing Using Optimization

The autopilot with distance optimization was implemented using the algorithm that has been realized and tested. The first



Fig. 17 New flight routes that have been compensated for by blank spots.



Fig. 18 Result of stitching using the developed autopilot system.

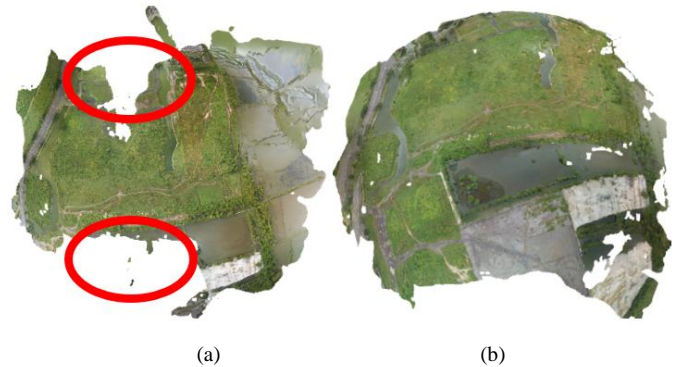


Fig. 19 Map of testing results, (a) conventional autopilot, (b) developed autopilot.

step was the same as that in the conventional system, namely entering the coordinates of the area coverage to be taken in aerial photography. However, the flight was done only once in this test since the blank spot analysis and flight route planning stages were carried out when the aircraft was still flying. The aerial photography parameters used were the same as the data in the conventional system test. Program optimization was performed by Python programs built and run in GCS. While the UAV was flying, the data were synchronized using the GCS for blank spot analysis and new flight route planning. Flight route

TABLE VI
STITCHING PROCESS FOR MAPPING FROM THE RESULTS OF THE DEVELOPED
AUTOPILOT SYSTEM

Order	Stages	Quality	Time (s)
1	Align photos	Low	262
2	Build dense cloud	Low	230
3	Build mesh	Low	373
4	Build texture	Low	90
5	Build tiled model	Low	1,800
6	Build orthomosaic	Low	337
7	Export orthomosaic		33
Total time			3,125

TABLE VII
TIME REQUIRED FOR MAPPING USING AUTOPILOT SYSTEM WITH OPTIMIZED
RESULTS SYSTEM

Parameter	Value on Mission 1
Flying time	161 seconds
Stitching time	3,125 seconds
Total	3,286 seconds
Battery capacity usage	2,100 mAh

records and blank spot analysis results in GCS are shown in Fig. 15.

The testing carried out showed two areas identified as blank spots, with coordinates on the canvas were (204, 384) and (116, 125). On earth, those points are at (-7.282783096, 112.8180628608) and (-7.280427749999999, 112.8172594032).

Next, a new flight route was created based on the blank spot location and the distance was optimized using the genetic algorithm. The parameters used are presented in Table V. The results of the distance optimization on the new flight route are shown in Fig. 16. After that, the autopilot created a new flight route, which was then merged with the old flight route, as shown in Fig. 17. Flight routes number 8 and 9 are flight routes used as compensation for blank spots.

Subsequently, the new flight mission arrangement was performed, as depicted in Fig. 17. The new flight mission had the same waypoint data as the primary flight mission but was added waypoint blank spot data obtained from the previous flight’s analysis result. Bearing that mission, the UAV would fly again and take off in the same direction as the previous flight.

UAV took 161 s to complete the entire mapping mission in this testing. The obtained photos entered the stitching phase, then the time required was calculated. The time required for the stitching process in this stage is shown in Table VI, the stitching results using the proposed autopilot system are shown in Fig. 18, while the time required for all stages and battery capacity is presented in Table VII.

C. Testing Results Comparison of the Conventional Autopilot and Developed Autopilot

After testing each autopilot, the results of photo processing between conventional autopilot and developed autopilot were compared. A comparison of maps is presented in Fig. 19. The results show that blank spots are found on the map with

conventional autopilot; the developed autopilot, on the other hand, generates perfect results. The conventional autopilot testing took 6,133 s, while the proposed autopilot took 3,286 s. Consequently, the developed autopilot reduced the time required for aerial photography by 46.4%.

V. CONCLUSION

Autopilot for aerial mapping with blank spot improvement and flight route optimization has been successfully developed and realized. The developed autopilot was able to reduce aerial photography time by 46.4% and save battery consumption by 41.18%. No blank spots were found on the map produced by the developed autopilot, whereas there were two blank spot locations on the map produced by the conventional autopilot. With the advantages of accelerated aerial photography time and battery capacity, the use of the developed autopilot saves operational costs.

CONFLICT OF INTEREST

The authors declare there is no conflict interest.

AUTHORS CONTRIBUTION

Ronny Mardiyanto serves as the lead researcher of the topic discussed in this paper, who also write this paper and initiates the idea to develop autopilot with distance optimization using the genetic algorithm. Muhammad Ichlasul Salik, as a research assistant, is in charge of making tools, creating program code, and conducting testing. Djoko Purwanto plays a role in providing suggestions related to the optimization algorithm used.

ACKNOWLEDGEMENT

The authors would like to thank the Ministry of Education, Culture, Research, and Technology for providing research funds through the 2021 Higher Education Excellence Basic Research (PDUPT) scheme.

REFERENCES

- [1] H. Gularso, S. Subiyanto, and L.M. Sabri, “Tinjauan Pemotretan Udara Format Kecil Menggunakan Pesawat Modelskywalker 1680 (Studi Kasus: Area Sekitar Kampus Undip),” *J. Geodesi Undip*, Vol. 2, No. 2, pp. 78-94, Apr. 2013.
- [2] R. Mardiyanto, R. Hidayat, E. Aprilian, and H. Suryoatmojo, “Development of Autopilot System of Unmanned Aerial Vehicle for Aerial Mapping Application,” *2018 Int. Sem. Intell. Technol., Its Appl. (I.S.I.T.I.A.)*, 2018, pp. 357–361.
- [3] A. Ahmad and A.M. Samad, “Aerial Mapping Using High Resolution Digital Camera and Unmanned Aerial Vehicle for Geographical Information System,” *2010 6th Int. Colloq. Signal Process., Its Appl.*, 2010, pp. 1–6.
- [4] K.N. Tahar, A. Ahmad, W.A.A.W.M. Akib, and W.M.N.W. Mohd, “Aerial Mapping Using Autonomous Fixed-Wing Unmanned Aerial Vehicle,” *2012 IEEE 8th Int. Colloq. Signal Process., Its Appl.*, 2012, pp. 164-168.
- [5] (2020) “Pixhawk Overview — Copter Documentation,” [Online], <http://ardupilot.org/copter/docs/common-pixhawk-overview.html>, access date: 20-Nov-2020.
- [6] A.P. Engelbrecht, *Fundamentals of Computational Swarm Intelligence*. Hoboken, AS: Wiley, 2005.

- [7] K. Krisnandi and H. Agung, "Implementasi Algoritma Genetika untuk Memprediksi Waktu dan Biaya Pengerjaan Proyek Konstruksi," *J. Ilm. FIFO*, Vol. 9, No. 2, pp. 90–97, 2017.
- [8] D. Sundarningsih, "Penerapan Algoritma Genetika untuk Optimasi Vehicle Routing Problem with Time Window (VRPTW): Studi Kasus Air Minum Kemasan," Undergraduate Thesis, Universitas Brawijaya, Malang, Indonesia, Jan. 2015.
- [9] D.M. Pierre, N. Zakaria, and A.J. Pal, "Master-Slave Parallel Vector-Evaluated Genetic Algorithm for Unmanned Aerial Vehicle's Path Planning," *2011 11th Int. Conf. Hybrid Intell. Syst. (HIS)*, 2011, pp. 517–521.
- [10] Z. Cheng and D. Li, "Improved G.A.S.A. Algorithm for Mutation Strategy UAV Path Planning," *2018 10th Int. Conf. Commun. Softw., Netw. (ICCSN)*, 2018, pp. 506–510.
- [11] Z. Cheng, Y. Sun, and Y. Liu, "Path Planning Based on Immune Genetic Algorithm for UAV," *2011 Int. Conf. Electric Inf., Control Eng.*, 2011, pp. 590–593.
- [12] Y.V. Pehlivanoglu and A. Hacıoglu, "Vibrational Genetic Algorithm Based Path Planner for Autonomous UAV in Spatial Data Based Environments," *2007 3rd Int. Conf. Recent Adv. Space Technol.*, 2007, pp. 573–578.
- [13] M. Cakir, "2D Path Planning of UAVs with Genetic Algorithm in a Constrained Environment," *2015 6th Int. Conf. Model., Simul., Appl. Optim. (ICMSAO)*, 2015, pp. 1–5.
- [14] J.A. Gonçalves and R. Henriques, "UAV Photogrammetry for Topographic Monitoring of Coastal Areas," *ISPRS J. Photogramm. Remote Sens.*, Vol. 104, pp. 101–111, Jun. 2015.